International Journal of Mathematical Archive-3(11), 2012, 4004-4016
Available online through www.ijma.info ISSN 2229 – 5046

INFLUENCE OF PARTIAL SLIP ON THE PERISTALTIC TRANSPORT OF A MICROPOLAR FLUID IN AN INCLINED ASYMMETRIC CHANNEL

M. Arun Kumar[1], S. Venkataramana[1], S. Sreenadh[2] and P. Lakshminarayana[2*]

[1,2]Department of Mathematics, S V University, Tirupati-517 502, A.P., India
[2]Department of Mathematics, Sree Vidyanikethan Engineering college Tirupati-517 02, A.P, India*

(Received on: 24-10-12; Revised & Accepted on: 28-11-12)

ABSTRACT

E*ffect of slip on the peristaltic transport of a micropolar fluid in an inclined asymmetric channel has been studied under the assumptions of long-wavelength and low-Reynolds number. The analytical solution has been derived for the axial velocity, microrotation component. Expressions for the pressure rise, stream function and the shear stress are also obtained. The effects of pertinent parameters on the pressure rise per wavelength are evaluated numerically. The phenomenon of trapping is also discussed.*

Keywords: *Peristaltic transport, Micropolar fluid, partial slip, Inclined Asymmetric channel.*

1. INTRODUCTION

The peristaltic pumping is a form of material transport generated by a progressive wave of area contraction or expansion along the length of a distensible tube, mixing and transporting the fluid in the direction of the wave propagation. In the living systems peristalsis plays an indispensable role in transporting many physiological fluids in various situations such as swallowing of foodstuffs through esophagus and the vasomotion of small blood vessels, urine transport from kidney to bladder, transport of spermatozoa in the ducts efferentes of the male reproductive tract.

Engineers designed many modern mechanical devices having industrial and physiological applications adapting the principle of peristalsis. The problem of the mechanism of peristaltic transport has attracted the attention of many investigators since the first investigation of Latham [1]. A number of analytical, numerical and experimental studies of peristaltic flow of different fluids have been reported under different conditions with reference to physiological and mechanical situations ([10]-[13]).

Some of the biofluids like water can be treated as newtonan. But there are many biofluids (eg: blood) whose behavior can not be described by the Newtonian's law of velocity. The inadequacy of the theory of Newtonian fluids in predicting the behavior of some fluids, especially those of high molecular weight leads to the development of non-Newtonian fluid mechanics. Hence some investigators have recently engaged in making progress in peristaltic flows of non-Newtonian fluids. It is realized that the model of micropolar fluid introduced by Eringen [2] serves as an appropriate model for blood. These fluids consist of rigid, randomly oriented (or spherical) particles suspended in a viscous medium where the deformation of particles is ignored. Basically, these fluids can support couple stresses and body couples and exhibit micro rotational and micro inertial effects. It can be observed that micropolar fluid model takes care of the rotation of fluid particles by means of an independent kinematic vector called micro rotation vector. Therefore, the model of a micropolar fluid may be more appropriate for any bio-fluids. Lukasazewicz [3] discussed many important aspects of the theory and applications of micropolar fluids. Devi and Devanathan [4] studied the peristaltic motion of a micropolar fluid in a cylindrical tube. Srinivasacharya et al. [5] analyzed the peristaltic transport of a micropolar fluid in a tube.

In several applications, the flow pattern corresponds to a slip flow and the fluid presents a loss of adhesion at the wetted wall making the fluid slide along the wall. When the molecular mean free-path length of the fluid is comparable to the distance between the plates (nanochannels or micro channels), the fluid exhibits non-continuum effects such as slip flow. Flows with slip would be useful for problems in chemical engineering, for example, flows through pipes in which chemical reactions occur at the walls, two-phase flows in porous slider bearings. Hayat et al. [6] have investigated the peristaltic transport of Maxwell fluid with slip through porous medium.

Corresponding author: *S. Sreenadh[2]*
[1,2]Department of Mathematics, S V University, Tirupati-517 502, A.P., INDIA

It is observed that all biological systems are not symmetric ducts. In view of this fact , some of the investigators studied the fluid flows in asymmetric channels. Mishra and Ramachandra Rao [7] studied the peristaltic transport of a Newtonian fluid in an asymmetric channel. It is known that many ducts in physiological systems are not horizontal but have some inclination with axis. Hence, Vajravelu et al. [8] studied the peristaltic transport of a Herschel-Bulkely fluid in an inclined tube. Srinivas and Pushparaj [9] studied peristaltic transport in an inclined asymmetric channel

Motivated by the above investigations, the effect of slip on the peristaltic transport of a micropolar fluid in an inclined asymmetric channel has been studied under long wave length and low Reynolds number assumptions. Applying wave frame analysis, exact analytic solutions have been obtained for the axial velocity and the microrotation component. Expressions for the pressure rise, the stream function and the shear stress are also obtained.

2. MATHEMATICAL SOLUTION

Consider the flow of an incompressible micropolar fluid in an inclined asymmetric channel of width $d_1 + d_2$. The flow in the channel is governed by micropolar model. The flow is induced by sinusoidal wave trains propagating with constant speed c along the channel wall. The geometry of the walls surfaces is

$$\overline{h_1}(\bar{x},\bar{t}) = d_1 + a_1 \cos\left(\frac{2\pi}{\lambda}\left(\bar{x} - c\bar{t}\right)\right) \text{ ----- (upper wall)} \tag{1}$$

$$\overline{h_2}\left(\bar{x},\bar{t}\right) = -d_2 - a_2 \cos\left(\frac{2\pi}{\lambda}\left(\bar{x} - c\bar{t}\right) + \varphi\right) \text{----- (lower wall)} \tag{2}$$

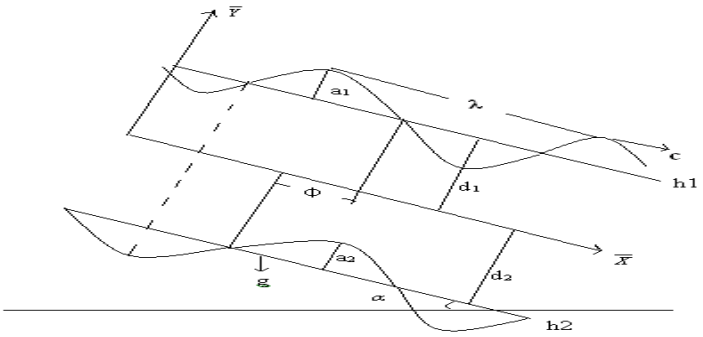

Figure 1: Physical Modal

where a_1 and a_2 are the amplitudes of the waves, λ is the wave length, c is the wave speed, $\phi\left(0 \le \phi \le \pi\right)$ is the phase difference, $\overline{X}$ and $\overline{Y}$ are the rectangular coordinates with $\overline{X}$ measured along the axis of the channel and $\overline{Y}$ perpendicular to $\overline{X}$. Let $\left(\overline{U},\overline{V}\right)$ be the velocity components in a fixed frame of reference $\left(\overline{X},\overline{Y}\right)$. It should be noted that $\phi = 0$ corresponds to a symmetric channel with waves out of phase and for $\phi = \pi$ the waves are in phase .

In the laboratory frame $\left(\overline{X},\overline{Y}\right)$ the flow is unsteady. However it is observed in a coordinate system $\left(\bar{x},\bar{y}\right)$ moving at the wave speed c, the flow can be treated as steady. The coordinates and velocities in the wave and lab frames related through the following expressions:

$$\bar{x} = \overline{X} - c\bar{t}, \quad \bar{y} = \overline{Y}, \quad \bar{u}\left(\bar{x},\bar{y}\right) = \overline{U} - c, \quad \bar{v}\left(\bar{u},\bar{v}\right) = \overline{V} \tag{3}$$

where $\bar{u}$ and $\bar{v}$ are the velocity components in the wave frame .

Neglecting body force and body couple, the equations governing the steady flow of an incompressible micropolar fluid are

$$\nabla.\bar{v} = 0 \tag{4}$$

$$\rho\left(\bar{v}.\nabla\right)\bar{v} = -\nabla\bar{p} + k\nabla\times\bar{w} + \left(\mu + k\right)\nabla^2\bar{v} \tag{5}$$

$$\rho\bar{j}\left(\bar{v}.\nabla\right)\bar{w} = -2k\bar{w} + k\nabla\times\bar{v} - \gamma(\nabla\times\nabla\times\bar{w}) + (\alpha+\beta+\gamma)\nabla(\nabla.\bar{w}) \tag{6}$$

where $\bar{v}$ is the velocity vector, $\bar{w}$ is the microrotation vector, $\bar{p}$ is the fluid pressure, ρ and $\bar{j}$ are the fluid density and microgyration parameter. Further, the material constants $\mu, k, \alpha \ \ and \ \ \gamma$ satisfy the following inequalities

$$2\mu + k \geq 0, \quad k \geq 0, \qquad 3\alpha + \beta + \gamma \geq 0, \quad \gamma \geq \left|\beta\right| \tag{7}$$

For the flow under consideration, the velocity field is $\bar{v} = \left(\bar{u}, \bar{v}, 0\right)$ and micro rotation vector is $\bar{w} = \left(0, 0, \bar{w}\right)$. We introduce the following non-dimensional quantities:

$$\begin{gathered} x = \frac{\bar{x}}{\lambda}, \quad y = \frac{\bar{y}}{d_1}, \quad u = \frac{\bar{u}}{c}, \quad v = \frac{\lambda\bar{v}}{d_1 c}, \quad w = \frac{d_1\bar{w}}{c}, \quad t = \frac{c}{\lambda}\bar{t}, \quad j = \frac{\bar{j}}{{d_1}^2} \\ h_1 = \frac{\bar{h_1}}{d^1}, \ h_2 = \frac{\bar{h_2}}{d^1}, \quad \delta = \frac{d_1}{\lambda}, \quad \mathrm{Re} = \frac{\rho c d_1}{\mu}, \ p = \frac{{d_1}^2}{c\lambda\mu}\bar{p}, \eta = \frac{{d_1}^2\rho g}{c\mu_0} \end{gathered} \tag{8}$$

where Re is the Reynolds number, δ is the dimensionless wave number and p is the pressure.

Using long wavelength and low Reynolds number approximations, the governing quantities in dimensionless form can be written as

$$\frac{\partial u}{\partial x} + \frac{\partial u}{\partial y} = 0 \tag{9}$$

$$\frac{\partial^2 u}{\partial y^2} = (1-N)\frac{\partial p}{\partial x} - N\frac{\partial w}{\partial y} - \eta\sin\alpha \tag{10}$$

$$\frac{\partial p}{\partial y} = 0 \tag{11}$$

$$-2w - \frac{\partial u}{\partial y} + \frac{(2-N)}{m^2}\frac{\partial^2 w}{\partial y^2} = 0 \tag{12}$$

where $N = \dfrac{k}{\mu + k}$, is the coupling number $\left(0 \leq N \leq 1\right)$, $m^2 = {d_1}^2 k\left(2\mu + k\right)/\left(\gamma\left(\mu + k\right)\right)$ is the micropolar parameter and α, β do not appear in the governing equations as the microrotation vector is solenoidal. These equations reduce to the classical Navier-Stokes equations when $k \to 0$.

The dimensional volume flow rate in the laboratory frame is

$$Q = \int_{\bar{h_2}\left(\bar{X},\bar{t}\right)}^{\bar{h_1}\left(\bar{X},\bar{t}\right)} \bar{U}\left(\bar{X},\bar{Y},\bar{t}\right)d\bar{Y} \tag{13}$$

In the wave frame the above equation reduces to

$$q = \int_{\bar{h_2}\left(\bar{x}\right)}^{\bar{h_1}\left(\bar{x}\right)} u\left(\bar{x},\bar{y}\right)d\bar{y} \tag{14}$$

From equations (3), (17) and (18), we get

$$Q = q + c\overline{h_1}\left(\overline{x}\right) - c\overline{h_2}\left(\overline{x}\right) \tag{15}$$

The time averaged flow over a period T at a fixed position X^1 is

$$\overline{Q} = \frac{1}{T}\int_0^T Q\,dt \tag{16}$$

Using (19) in (20) and then integrating we get

$$\overline{Q} = q + cd_1 + cd_2 \tag{17}$$

Defining the dimensionless mean flow Θ in the laboratory frame and F in the wave frame as

$$\Theta = \frac{\overline{Q}}{c\overline{d_1}}, \quad F = \frac{q}{c\overline{d_1}} \tag{18}$$

Equation (21) reduces to

$$\Theta = F + 1 + d \tag{19}$$

in which

$$F = \int_{h_2}^{h_1} u\,dy \tag{20}$$

The dimensionless forms of the permeable surfaces of the peristaltic walls are

$$h_1(x) = 1 + a\cos(2\pi x), \quad h_2(x) = -d - b\cos(2\pi x + \phi) \tag{21}$$

where $a = \frac{a_1}{d_1}$, $b = \frac{a_2}{d_1}$ *and* $d = \frac{d_2}{d_1}$

In the wave frame the boundary conditions are

$$u + L\frac{\partial u}{\partial y} = -1 \quad at \quad y = h_1 \text{ (upper wall)}$$

$$u - L\frac{\partial u}{\partial y} = -1 \quad at \quad y = h_2 \text{ (lower wall)} \tag{22}$$

$$w = -L\frac{\partial w}{\partial y} \quad at \quad y = h_1$$

$$w = L\frac{\partial w}{\partial y} \quad at \quad y = h_2 \tag{23}$$

3. SOLUTION OF THE PROBLEM

From the equation (10) we obtain

$$\frac{\partial u}{\partial y} = \left((1-N)\frac{\partial p}{\partial x} - \eta\sin\alpha\right)y - Nw + c_1 \tag{24}$$

Using the equations (11) and (24) in (12) we get

$$-2w - \left((1-N)\frac{dp}{dx} - \eta\sin\alpha\right)y + Nw - c_1 + \frac{(2-N)}{m^2}\frac{\partial^2 w}{\partial y^2} = 0 \tag{25}$$

Solving the equation (25) and write

$$w = c_2 \cosh my + c_3 \sinh my - \frac{\chi^2}{m^2}\left(\frac{dp}{dx}(1-N)y - \eta \sin\alpha + c_1\right) \tag{26}$$

Solving the equation (24) by using (26) and the boundary conditions (22) and (23) we obtain

$$u = \left((1-N)\frac{dp}{dx} - \eta \sin\alpha\right)a_1 \frac{y^2}{2} + c_1 a_1 y - \frac{N}{m}\left(c_2 \sinh my + c_3 \cosh my\right) + c_4 \tag{27}$$

From equation (20) we find that

$$\frac{d}{d} = \frac{F + (a51 - a52 + a53)}{x(a48 - a49 + a50)} = \frac{\Theta - 1 - d + (a51 - a52 + a53)}{(a48 - a49 + a50)} \tag{28}$$

The corresponding stream function is

$$\psi = \left((1-N)\frac{dp}{dx} - \eta \sin\alpha\right)a_1 \frac{y^3}{6} + c_1 a_1 \frac{y^2}{2} - \frac{N}{m^2}\left(c_2 \cosh my + c_3 \sinh my\right) + c_4 y \tag{29}$$

The non-dimensional form of the pressure rise per wavelength ΔP is given by

$$\Delta P = \int_0^1 \left(\frac{dp}{dx}\right) dx \tag{30}$$

Shear stress distribution at the walls

An important property of the micropolar fluid is that the stress tensor is not symmetric. The non-dimensional shear stresses in the problem under consideration are given by

$$\tau_{xy} = \frac{\partial u}{\partial y} - \frac{N}{1-N} w \tag{31}$$

$$\tau_{yx} = \frac{1}{1-N}\frac{\partial u}{\partial y} + \frac{N}{1-N} w \tag{32}$$

4. RESULTS AND DISCUSION

Velocity has been calculated as a function of y from the equation (27) and plotted in figure.2 to study the effects of different parameters such as coupling number N, microrotation parameter m, pressure gradient P, slip parameter L and α on the velocity distribution. From Fig.2a and Fig.2b we observe that the velocity increases with increasing a and b. Fig.2c and Fig.2d shows that velocity decreases with increasing m and N. From Fig.2e and Fig.2f we observe that the velocity increases with increasing L and α.

We have calculated the pressure rise Δp in terms of the mean flow Θ from equation (30). The variation of pressure rise with the mean flow for different values of m is shown in Fig.3a. It is noticed that the pressure rise decreases with the increase in Θ. We observe that for a given Θ, pressure rise decreases with increasing m. Also for fixed Δp, the increase in m decreases the mean flow. The variation of pressure rise with the mean flow for different N is shown in Fig.3b. We notice that for a given Θ, pressure rise increases with increasing N. Also for fixed Δp, the increase in N increases the mean flow. Fig.3c shows the variation of pressure rise with the mean flow for different values of ϕ. We find that for fixed Θ, pressure rise decreases with increasing ϕ. Also for a given Δp, the increase in ϕ decreases the mean flow. The variation of pressure rise with the mean flow for different values of slip parameter L is shown in Fig.3d. We observe that the pumping curves are intersect at a point between Θ =0.4 and Θ =0.6. Above this point ΔP decreases with increasing L and below the intersecting point opposite behavior can be identified. Fig.3e

shows the variation of pressure rise with the mean flow for different values of α .We observe that for a given Θ, pressure rise increases with increasing α . Also for fixed Δp, the increase in α increases the mean flow.

Since the expressions for τ_{xy} and τ_{yx} are different, it is clear that stress tensor is not symmetric in micropolar fluid. Fig.4a is drawn to study the effect of m on shear stress τ_{xy} at the upper wall for a symmetric channel. We observe that shear stress is symmetric about x = 0. Also it decreases with increase in m . It is noticed that the shear stress has direction opposite to the upper wave velocity. Fig.4b shows the effect of N for an asymmetric channel. It is noticed that the shear stress decreases at the ends of the channel and increase in midway of the channel with increase in N . Fig.4c is plotted to study the effect of L on shear stress τ_{xy} at the upper wall for an asymmetric channel. We observe that shear stress increases with increase in L . From fig.4d it is found that the shear stress τ_{xy} at the upper wall decreases for increasing α with $\phi = \pi/2$.

Fig.5a is drawn to observe the effect of m on shear stress τ_{yx} at the lower wall for a symmetric channel. It is noticed that the shear stress decreases with increase in m . Fig.5b is plotted to study the effect of N on shear stress τ_{yx} at the lower wall for a symmetric channel. It is observed that the shear stress increases with increase in N . Fig.5c shows the effect of L on shear stress τ_{yx} at the lower wall for an asymmetric channel. We observe that shear stress decreases with increase in L . From fig.5d it is noticed that the shear stress τ_{yx} at the lower wall increases for increasing α $\phi = \pi/2$.

The formation of an internally circulating bolus of fluid by closed streamlines is called trapping and this trapped bolus is pushed ahead along with the peristaltic wave. The stream lines for different values m are plotted in Fig.6 It is observed that the size of bolus increases as m increases. The effect of N on trapping is illustrated in Fig.7. It can be seen that the size of bolus decreases with the increase of N . The stream lines for different values of L are plotted in Fig.8. We notice that the size of bolus increases with increasing L . The stream lines for different values α are plotted in Fig.9 It is observed that the size of bolus increases as α increases.

CONCLUSIONS

This study is made in order to explain the effect of slip on the peristaltic transport of a micropolar fluid in an inclined asymmetric channel. The effects of various emerging parameters on the axial velocity, pressure rise, shear stress and stream line flow pattern are seen with the help of graphs. From the present study the following conclusions can be drawn.

- The magnitude of the axial velocity increases at the boundaries and central part of the channel by increasing the slip parameter L .
- The magnitude of the axial velocity decreases at the boundaries and central part of the channel by increasing m and N .
- The pressure rise increases with the increase in N and α where as it decreases as m and ϕ increases.
- Shear stress τ_{xy} at the upper wall decreases with an increase in m in a symmetric channel, while it increases when L increases in an asymmetric channel.
- Shear stress τ_{yx} at the lower wall decreases in the mid way of the channel with an increase in m and increases when N is increased in a symmetric channel, while it increases with decreasing L and and increasing α in an asymmetric channel.
- The volume of the trapped bolus increases with increase in m , L and α while it decreases with an increase in N .

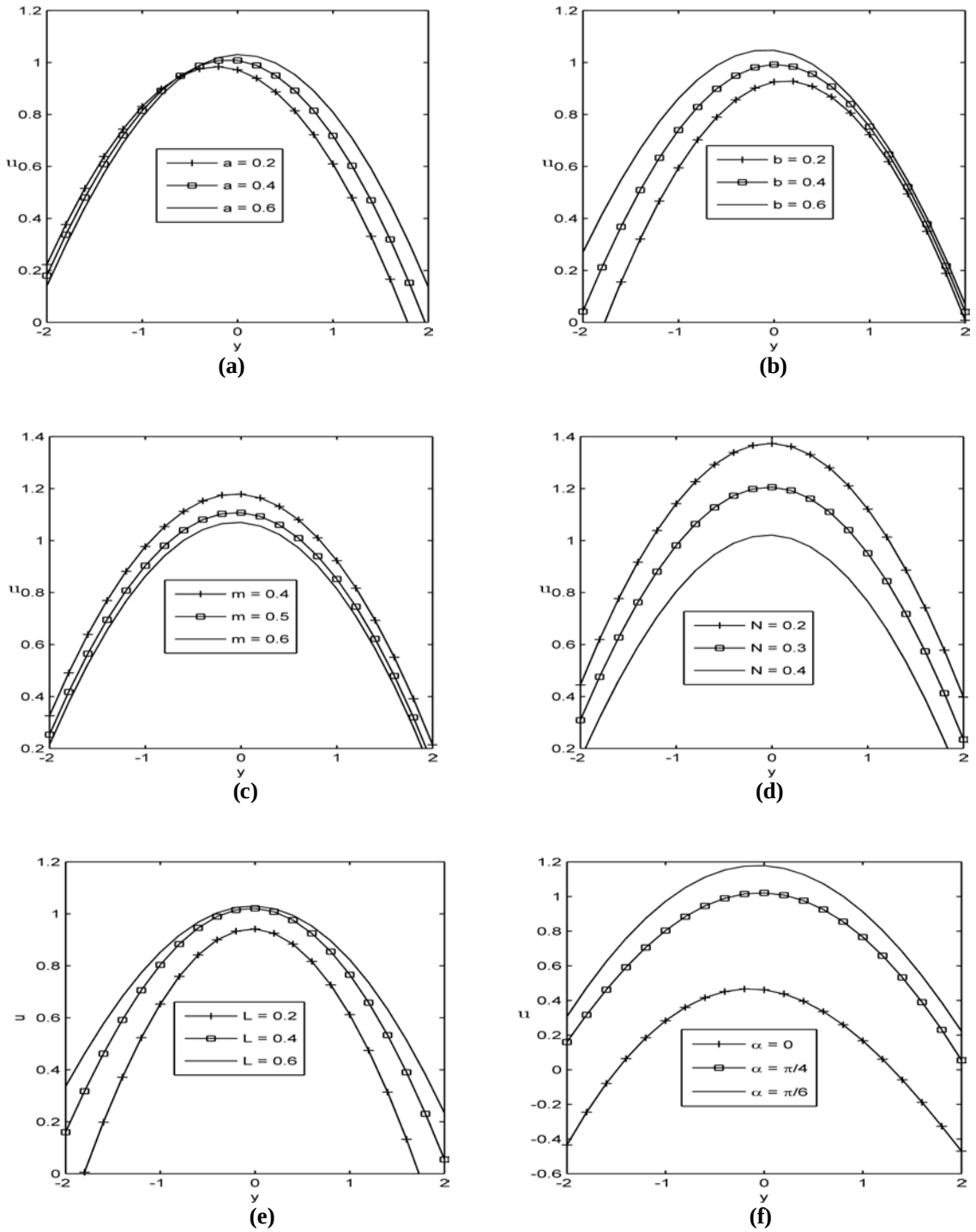

Fig 2. Velocity distribution: $\mathrm{d}=1, \phi=0,\ \mathrm{x}\ =0, \eta=1, \Theta=1$

(a) $\mathrm{b}=0.5,\ \mathrm{N}=0.4,\ \mathrm{m}=1, \alpha=\pi/4, \phi=0, \mathrm{L}=0.4.$

(b) $a=0.5,\ \mathrm{N}=0.4,\ \mathrm{m}=1, \alpha=\pi/4,\ \phi=0, \mathrm{L}=0.4.$

(c) $a=0.5, \mathrm{b}=0.5,\ \mathrm{N}=0.4, \alpha=\pi/4, \phi=0, \mathrm{L}=0.4.$

(d) $a=0.5, \mathrm{b}=0.5,\ \mathrm{m}=1, \alpha=\pi/4, \phi=0, \mathrm{L}=0.4.$

(e) $a=0.5, \mathrm{b}=0.5,\ \mathrm{N}=0.4, \mathrm{m}=1, \alpha=\pi/4, \phi=0.$

(f) $a=0.5, \mathrm{b}=0.5,\ \mathrm{N}=0.4, \mathrm{m}=1, \mathrm{L}=0.4, \phi=0.$

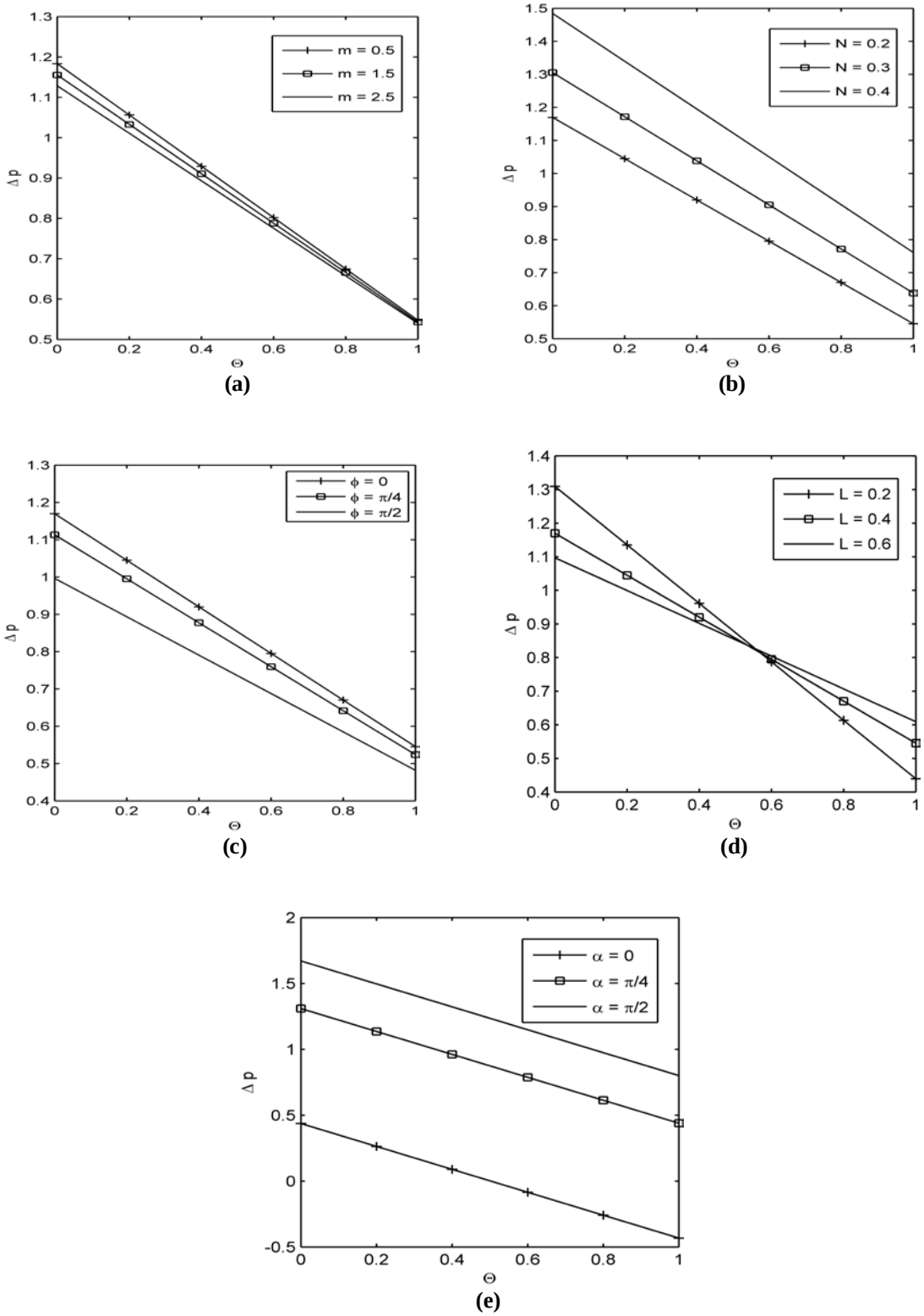

Fig 3. variation of Pressure rise: $a = 0.5, \mathrm{b} = 0.5, \mathrm{d} = 1.5, \eta = 1.$

(a) $\mathrm{N} = 0.2, \alpha = \pi/4, \phi = 0, L = 0.4$.

(b) $m = 1, \alpha = \pi/4, \phi = 0, L = 0.4$

(c) $\mathrm{N} = 0.2, m = 1, \quad \alpha = \pi/4, \ L = 0.4.$

(d) $\mathrm{N} = 0.2, m = 1, \alpha = \pi/4, \phi = 0.$

(e) $\mathrm{N} = 0.2, m = 1, L = 0.4, \phi = \pi/2.$

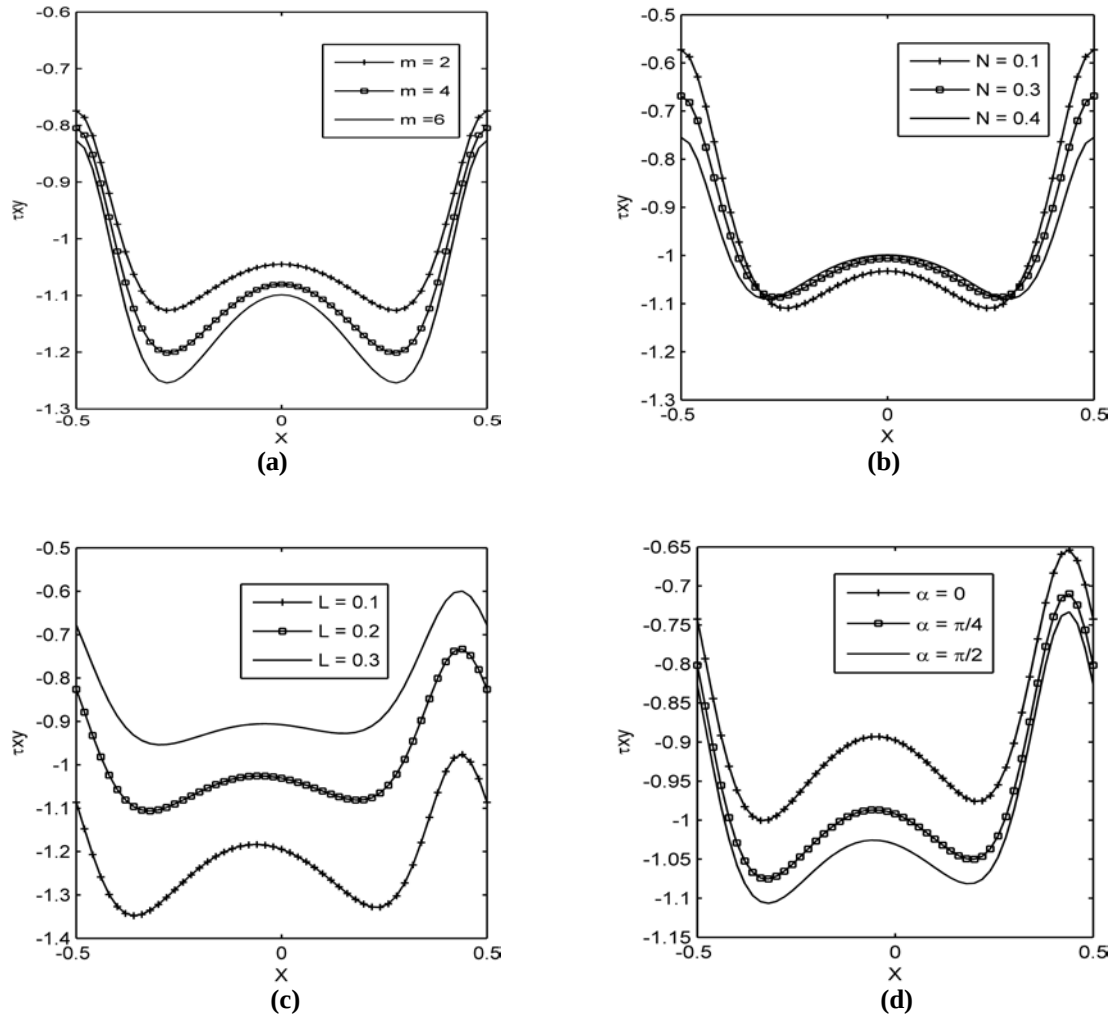

Fig 4. variation of shear stress τ_{xy} at the upper wall: $a = 0.5, b = 0.5,\ d = 1, \Theta = 1.2$

(a) $N = 0.2, \alpha = \pi/2, \phi = 0, L = 0.2.$

(b) $m = 1, \alpha = \pi/2, \phi = 0, L = 0.2.$

(c) $m = 1, N = 0.2, \phi = \pi/2, \alpha = \pi/2.$

(d) $m = 1, N = 0.2, \phi = \pi/2, L = 0.2.$

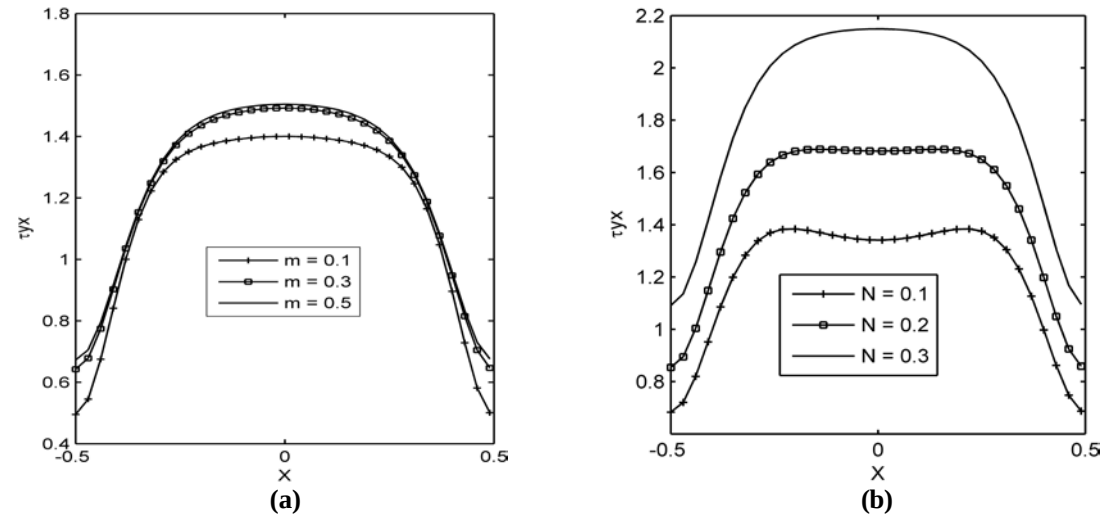

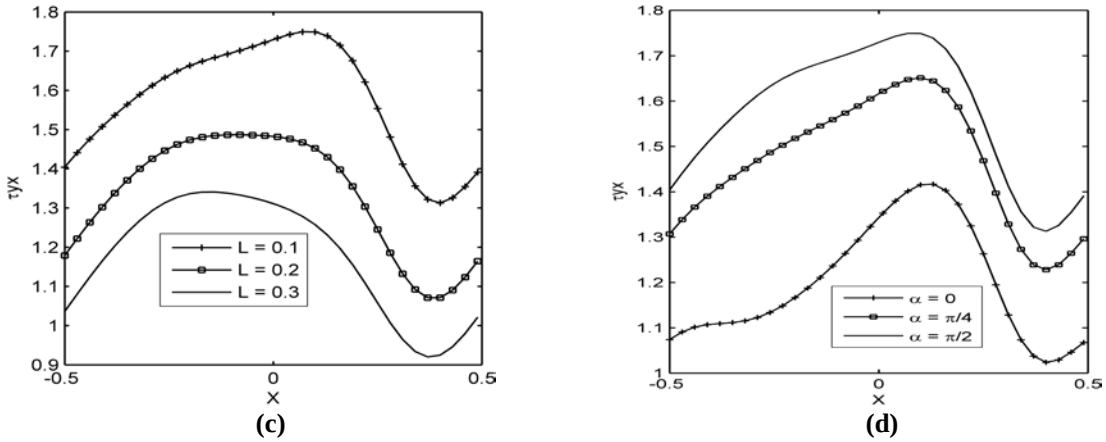

(c) **(d)**

Fig 5. variation of shear stress τ_{yx} at the lower wall: $a = 0.5, b = 0.5,\ d = 1.2, \Theta = 1.2$

(a) $N = 0.2, \alpha = \pi/2, \phi = 0, L = 0.2.$

(b) $m = 1, \alpha = \pi/2, \phi = 0, L = 0.1.$

(c) $m = 1, N = 0.2, \phi = \pi/2, \alpha = \pi/2.$

(d) $m = 1, N = 0.2, \phi = \pi/2, L = 0.1.$

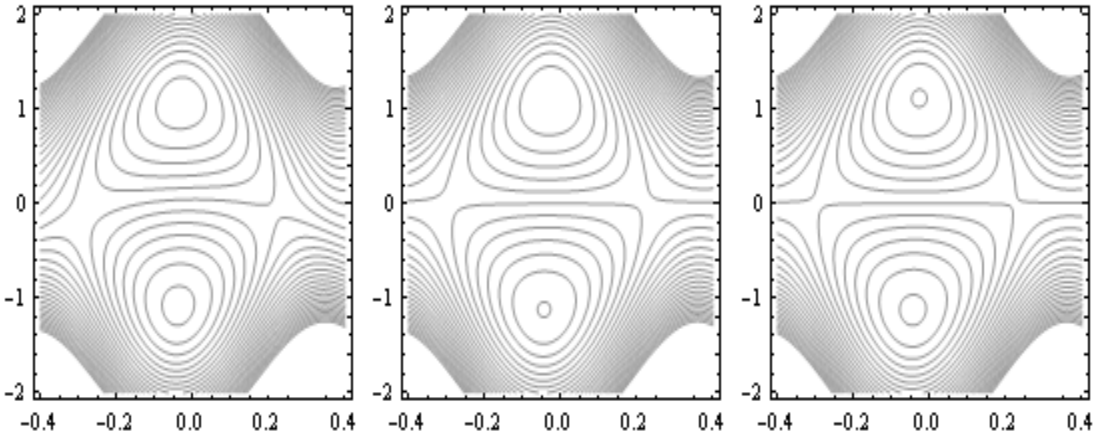

(a) **(b)** **(c)**

Fig 6. stream lines for (a) $m = 0.5$, (b) $m = 1$, (c) $m = 1.5$,
$a = 0.5, b = 0.5,\ N = 0.2, d = 1, \alpha = \pi/4, \phi = \pi/8,\ \eta = 1, L = 0.1, \Theta = 1.2$

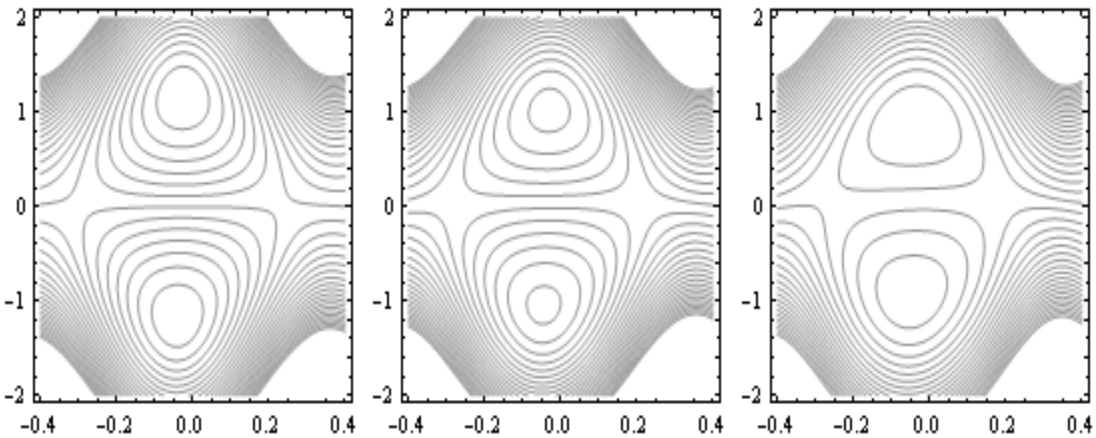

(a) **(b)** **(c)**

Fig 7. stream lines for (a) $N = 0.1$, (b) $N = 0.3$, (c) $N = 0.5$
$a = 0.5, b = 0.5,\ m = 1, d = 1, \alpha = \pi/4, \phi = \pi/8,\ \eta = 1, L = 0.1, \Theta = 1.2$

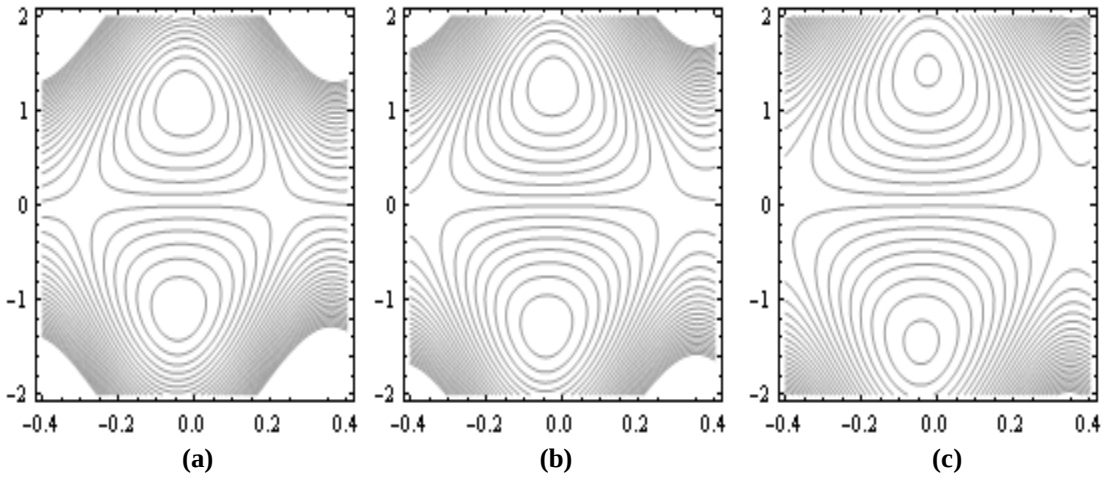

Fig 8. stream lines for (a) $L = 0.1$, (b) $L = 0.2$, (c) $L = 0.3$
$a = 0.5, b = 0.5,\ m = 1, N = 0.2, d = 1, \alpha = \pi/4, \phi = \pi/8,\ \eta = 1, \Theta = 1.2$

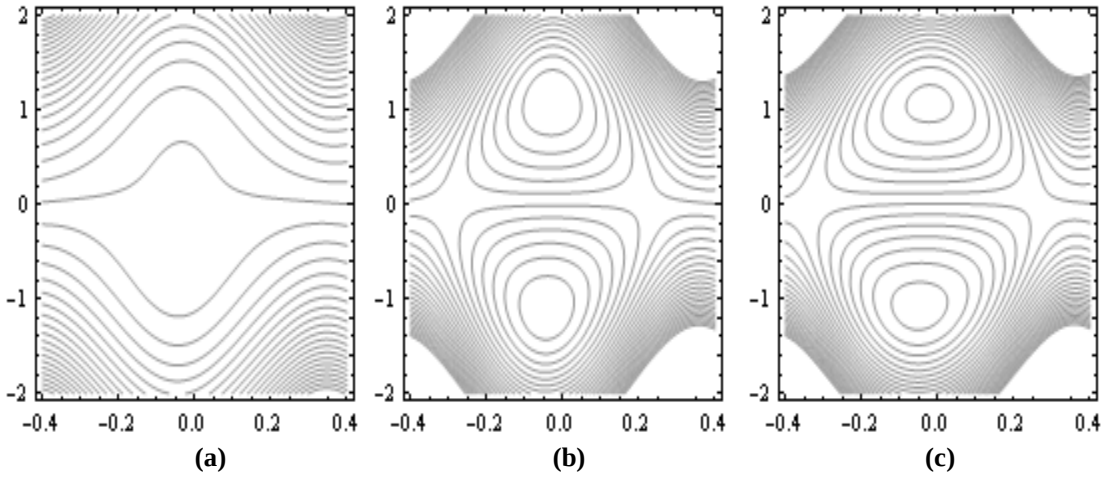

Fig 9. stream lines for (a) $\alpha = 0$, (b) $\alpha = \pi/4$, (c) $\alpha = \pi/2$
$a = 0.5, b = 0.5,\ N = 0.2, m = 1, d = 1, \phi = \pi/8,\ \eta = 1, L = 0.1, \Theta = 1.2$

ACKNOWLEDGEMENTS
One of the authors S. Sreenadh, expresses his grateful thanks to UGC authorities for providing financial support to undertake this work.

APPENDIX

$$\chi^2 = \frac{m^2}{2-N},\ a_1 = 1 + \frac{N\chi^2}{m^2},\ a_2 = a_1\left(\frac{h_1^2}{2} + Lh_1\right)$$

$$a_3 = a_2(1-N),\ a_4 = a_2\,\eta\sin\alpha,\ a_5 = N\left(\frac{\sinh mh_1}{m} + L\cosh mh_1\right)$$

$$a_6 = N\left(\frac{\cosh mh_1}{m} + L\sinh mh_1\right),\ a_7 = a_1(h_1 + L),\ a_8 = a_1\left(\frac{h_2^2}{2} - Lh_2\right)$$

$$a_9 = a_8(1-N),\ a_{10} = a_8\,\eta\sin\alpha,\ a_{11} = N\left(\frac{\sinh mh_2}{m} - L\cosh mh_2\right)$$

$$a_{12} = N\left(\frac{\cosh mh_2}{m} - L\sinh mh_2\right),\ a_{13} = a_1(h_2 - L),\ a_{14} = \cosh mh_1 + L\,m\sinh mh_1$$

$$a_{15} = \sinh mh_1 + L\,m\cosh mh_1,\ a_{16} = (1-N)\frac{\chi^2}{m^2}h_1(1+L),\ a_{17} = \eta\sin\alpha\frac{\chi^2}{m^2}h_1(1+L)$$

$$a_{18} = \frac{\chi^2}{m^2}(1+L),\ a_{19} = \cosh mh_2 - L\,m\sinh mh_2,\ a_{20} = \sinh mh_2 - L\,m\cosh mh_2$$

$$a_{21} = (1-N)\frac{\chi^2}{m^2}h_2(1-L),\ a_{22} = \eta\sin\alpha\frac{\chi^2}{m^2}h_2(1-L),\ a_{23} = \frac{\chi^2}{m^2}(1-L)$$

$$a_{24} = a_7 - a_{13},\ a_{25} = a_5 - a_{11},\ a_{26} = a_6 - a_{12},\ a_{27} = a_3 - a_9,\ a_{28} = a_4 - a_{10}$$

$$a_{29} = a_{14}\,a_{23} - a_{18}\,a_{19},\ a_{30} = a_{15}\,a_{23} - a_{20}\,a_{18},\ a_{31} = a_{16}\,a_{23} - a_{18}\,a_{21},\ a_{32} = a_{17}\,a_{23} - a_{18}\,a_{22}$$

$$a_{33} = a_{14}\,a_{24} - a_{18}\,a_{25},\ a_{34} = a_{15}\,a_{24} - a_{18}\,a_{26},\ a_{35} = a_{16}\,a_{24} - a_{18}\,a_{27},\ a_{36} = a_{17}\,a_{24} - a_{18}\,a_{28}$$

$$a_{37} = a_{30}\,a_{33} - a_{34}\,a_{29},\ a_{38} = a_{31}\,a_{33} - a_{35}\,a_{29},\ a_{39} = a_{32}\,a_{33} - a_{36}\,a_{29},\ a_{40} = \frac{a_{38}}{a_{37}},\ a_{41} = \frac{a_{39}}{a_{37}}$$

$$a_{42} = \frac{a_{35} - a_{40}}{a_{33}},\ a_{43} = \frac{a_{36} - a_{34}\,a_{41}}{a_{33}},\ a_{44} = \frac{a_{25}\,a_{42} + a_{26}\,a_{40} - a_{27}}{a_{24}} \qquad a_{45} = \frac{a_{43}\,a_{25} + a_{26}\,a_{41} - a_{28}}{a_{24}},$$

$$a_{46} = a_{42}\,a_{11} + a_{40}\,a_{12} - a_{44}\,a_{13} - a_9$$

$$a_{47} = a_{43}\,a_{11} + a_{41}\,a_{12} - a_{45}\,a_{13} - a_{10} + 1,\ a_{48} = \frac{a_1(1-N)\left(h_1^3 - h_2^3\right)}{6}$$

$$a_{49} = \frac{N}{m^2}\left[a_{42}\left(\cosh mh_1 - c\cosh mh_2\right) + a_{40}\left(\sinh mh_1 - \sinh mh_2\right)\right]$$

$$a_{50} = \frac{a_{44}\,a_1\left(h_1^2 - h_2^2\right)}{2} + a_{46}\left(h_1 - h_2\right),\ a_{51} = \frac{a_1\,\eta\sin\alpha\left(h_1^3 - h_2^3\right)}{6}$$

$$a_{52} = \frac{N}{m^2}\left[a_{43}\left(\cosh mh_1 - c\cosh mh_2\right) + a_{41}\left(\sinh mh_1 - \sinh mh_2\right)\right]$$

$$a_{53} = \frac{a_{45}\,a_1\left(h_1^2 - h_2^2\right)}{2} + a_{47}\left(h_1 - h_2\right)$$

REFERENCES

[1] Lathem, T.W., M.S. Thisis, M.I.T, (1966).

[2] Eringen, A.C., Theory of micropolar fluids. *J. Math. Mech.*, (1966), 16, pp. 1-16.

[3] Lukasazewicz, G., Micropolar fluid –Theory and Applications. Birkhausr, Boston.

[4] Devi, G. and Devanathan, R., Peristaltic motion of a micropolar fluid. *Proc. Indian Acad. Sci.*, (1975), 81 (A), pp. 149-163.

[5] Srinivasacharya, D., Mishra, M. and Rao, A.R., Peristaltic transport of a micripolar fluid in a tube. *Acta. Mech.*, (2003), 161, pp. 165-178.

[6] Hayat, T., Ali, N. and Asghar, S., Hall effects on peristaltic flow of a Maxwell fluid in a porous medium, Phys. Lett. A , (2007), 363, 397-403.

[7] Mishra, M., Ramachandra Rao, A., Peristaltic transport of a Newtonian fluid in an asymmetric channel, (2003), ZAMP, 54, 532-550.

[8] Vajravelu, K., Sreenadh, S. and Ramesh Babu, V., Peristaltic transport of a Hershel-Bulkley fluid in an inclined tube, Int. *J. Non-linear Mech.* (2005), 40, 83-90.

[9] Srinivas, S., Pushparaj, V., Non-linear peristaltic transport in an inclined asymmetric, *Commun. Non-linear Sci. Numer. Simul* (2008), 13, 1782-1795.

[10] Hayat, T. and Ali, N., Peristaltic motion of a Jeffrey fluid under the effect of a magnetic field in a tube, *Commun. Non-linear Sci. Numer. Simul*. (2008), 13, 1343-1352.

[11] Narahari, M. and Sreenadh, S. Peristaltic transport of a Bingham fluid in contact with a newtonian fluid. Int. J. of Appl. Math. and Mech. (2010). 6 (11), pp. 41-54.

[12] Ramana kumari, A.V., and Radhakrishnamacharya, G. Effect of slip on peristaltic transport in an inclined channel with wall effects. Int. J. of Appl. Math. and Mech. (2011). 7(1), pp. 1-14.

[13] Vajravelu, K. , Sreenadh, S. and Lakshminarayana, P. ,The influence of heat transfer on peristaltic transport of a Jeffrey fluid in a vertical porous stratum. Commun. Non- linear Sci. Numer. Simulat. (2011), 16, 3107-3125.

Source of support: Nil, Conflict of interest: None Declared

